



Modulation of neonatal growth plate development by *ex vivo* intermittent mechanical stress

Hasan Othman^a, Eugene J. Thonar^b, Jeremy J. Mao^{a,*}

^aDepartment of Biomedical Engineering, Fu Foundation School of Engineering and Applied Sciences, College of Dental Medicine, Columbia University, 630 W. 168 Street, PH7 East SDOS, New York, NY 10032, USA

^bDepartments of Biochemistry and Orthopaedics, Rush University, 1735 W. Harrison Street, Suite 526 Cohn Building, Chicago, IL 60612, USA

Accepted 14 December 2006

Abstract

Although growth plate response to mechanical stress has been increasingly studied, our understanding of mechanical modulation of neonatal growth plate is incomplete, especially concerning biochemical changes. This study was designed to explore the cellular and biochemical responses of the cranial base growth plate (CBGP) explant upon cyclic loading. The growth plate with subchondral bone was aseptically isolated from each of 24 neonatal rabbits and fixated in an organ culture system. Cyclic loading was applied to growth plate explants at 200 mN and 1 Hz for 60 min ($N = 12$), whereas control explants were immersed in organ culture for 60 min without mechanical loading ($N = 12$). Computerized image analysis revealed that cyclic loading induced significantly more proliferating chondrocytes than unloaded controls ($p < 0.001$), as well as significantly higher growth plate height at $856 \pm 30 \mu\text{m}$ than the unloaded controls at $830 \pm 36 \mu\text{m}$ ($p < 0.05$). Immunoblotting with monoclonal antibodies (mAb) disclosed that the average mAb binding area for chondroitin sulfate was significantly higher in the loaded specimens than the unloaded controls at ($p < 0.001$). The average mAb binding area for keratan sulfate was also significantly higher in the loaded specimens than the unloaded controls ($p < 0.01$). Biochemical analysis showed that the average total hyaluronan content of loaded specimens at $0.25 \pm 0.06 \mu\text{g}/\mu\text{g}$ DNA was significantly higher than the unloaded controls at $0.09 \pm 0.05 \mu\text{g}/\mu\text{g}$ DNA ($p < 0.01$). Taken together, these data suggest that brief doses of cyclic, intermittent forces activate cellular and molecular responses in the CBGP *ex vivo*. Whether hyaluronan-mediated pathway is involved in the biological responses of growth plate to mechanical loading warrants additional investigations.

© 2007 Published by Elsevier Ltd.

Keywords: Chondrocytes; Growth plate; Cartilage; Osteoblasts; Bone; Cyclic loading

1. Introduction

The cranial base growth plate (CBGP), or the sphenoccipital synchondrosis, is the only growth plate in the craniofacial skeleton that remains functionally viable postnatally up to the adolescent age and prior to the completion of craniofacial growth (Baume, 1961; Ingervall and Thilander, 1972). Morphologically, the CBGP consists of two growth plates with their reserve zones merged in the center, therefore enabling endochondral ossification in opposite directions, leading to continuous formation of the sphenoid and occipital bones (Baume, 1954). Premature

arrest of the CBGP leads to visible craniofacial anomalies (Hoyte, 1991; Rosenberg et al., 1997). Despite its importance in craniofacial development, little is known about the biology of the CBGP beyond its histological structure (Mao, 2005).

Chondral growth of the cranial base, like appendicular growth plates, relies on chondrocyte proliferation, differentiation and the synthesis of chondral matrices, in addition to concurrent vascular invasion and osteogenesis. The CBGP is considered to be controlled by genetically coded cycles of mitosis with no contribution from mechanical stimuli (Scott, 1958; Baume, 1970; Peltomaki et al., 1997; Proffit et al., 2000). Recent experimental data have demonstrated that chondral growth of the CBGP *in vivo* is modulated by brief doses of cyclic forces,

*Corresponding author. Tel.: +1 212 305 4475; fax: +1 212 342 0199.
 E-mail address: jmao@columbia.edu (J.J. Mao).

as compared to both static forces of matching peak magnitude and native chondral growth (Wang and Mao, 2002a). BrdU labeling shows that chondrocytes increase proliferation rates upon cyclic loading (Wang and Mao, 2002b), similar to observations in appendicular growth plates (Farnum et al., 2000, 2003; Stokes et al., 2002). Mechanical modulation of CBGF is similar to parallel models of *in vivo* mechanical loading of the appendicular growth plates (Robling et al., 2001; Ohashi et al., 2002; Stokes et al., 2002), although the magnitude of cyclic loading often differs substantially among these studies. The mechanical properties of the CBGP and the pericellular and interterritorial matrices have recently been investigated (Allen and Mao, 2004; Radhakrishnan and Mao, 2004) and are compatible with those of the appendicular growth plates, indicating the capacity of the CBGP to withstand mechanical stress.

Our understanding of growth plates has evolved mostly around developmental studies that describe their structure at various levels of organization (Kirsch et al., 1997; Alini and Roughley, 2001; Van der Eerden et al., 2003; Nilsson and Baron, 2004). Only in recent years has due attention been paid to the role of mechanical stress in the development of growth plates (Carter et al., 1998; Grodzinsky et al., 2000; Elder et al., 2001; Robling et al., 2001; Ohashi et al., 2002; Stokes et al., 2002, 2005; Wang and Mao, 2002a, b; Mao and Nah, 2004). Several types of mechanical stresses such as shear stresses and hydrostatic pressure have been proposed or shown to modulate the development of growth plates (Klein-Nulend et al., 1986; Carter et al., 1998; Tanck et al., 1999; Sundaramurthy and Mao, 2006). However, little is known of biochemical changes in the neonatal growth plate during normal development or upon mechanical loading. The objective of the present study was to explore the cellular and

biochemical changes in the isolated neonatal CBGP in organ culture upon cyclic loading.

2. Materials and Methods

2.1. Animal model and tissue harvesting

A total of 24 five-day old New Zealand White rabbits were randomly divided into control and experimental groups and euthanized by intracardiac injection of 100 mg/kg Euthasol (Delmarva Laboratories, Dallas, TX). The CBGP was aseptically isolated with approximately 4.5 mm of subchondral bone (Fig. 1a), and immediately placed in an organ culture chamber with Dulbecco's Modified Eagle Medium (DMEM) supplemented with 10% heat inactivated fetal bovine serum (FBS), and 1% Penicillin–streptomycin–L-glutamine. The dimensions of the CBGP explant were $5 \times 4 \times 10$ mm ($l \times w \times h$) Fig. 1b. The rabbit was selected as the animal model over rats or mice, because the neonatal rabbit has the appropriate CBGP size that can be manipulated *ex vivo*. The animal procedures were approved by the IACUC committee.

2.2. Mechanical loading

The bone end of the loaded explant was rigidly fixated and submerged in the culture medium (Fig. 1c). Compressive forces with a sinusoidal waveform at 200 mN, leading to approximately 10% strain and approximately 26.67 mN/mm^2 stress, and 1 Hz were applied to the subchondral bone and CBGP for a total of 60 min, resulting in 3600 loading cycles (858 Mini Bionix II, MTS, Eden Prairie, MN) (Fig. 1c). The force direction was anterior–posterior or axial as shown in Fig. 1a, or along the longitudinal axis of the loading platen as in Fig. 1c. These force magnitude and frequencies were selected on the basis of similar force parameters used in our previous studies of mechanical modulation of cranial sutures (Wang and Mao, 2002a, b; Kopher and Mao, 1999; Mao et al., 1998; Collins et al., 2005; Tang and Mao, 2006), as well as a companion study of mechanical modulation of neonatal distal femoral epiphysis (Sundaramurthy and Mao, 2006). During the 60 min loading period, the control explant was placed separately in identical organ culture medium, but without any exogenous mechanical loading. During the 60 min loading period, the explants were immersed in organ culture at room temperature. Once mechanical loading was completed, both the

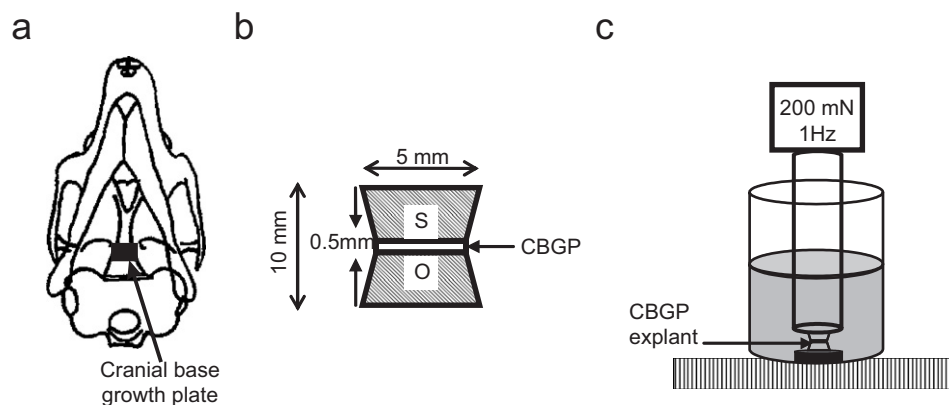


Fig. 1. Anatomical structure of the cranial base growth plate (CBGP) and setup for cyclic loading. (a) The cranial base growth plate (dark rectangle) in the posterior portion of the cranial base. The bone ventral (anterior) to the CBGP is sphenoid, whereas the bone dorsal (posterior) to the CBGP is occipital. (b) Schematic diagram of the isolated explant of the CBGP with approximately 4.5 mm of bone on both the sphenoid (S) and occipital (O) side. The CBGP in (a) was isolated in the same orientation without any rotation and is illustrated in (b). The CBGP is characterized by two growth plates merged by their reserve zones, and with two hypertrophic zones separately in the sphenoid (S) and occipital (O) bones. The CBGP thus possesses bidirectional growth potential, contributing to the elongation of both the sphenoid and occipital bones. (c) The CBGP in B is fixated in the same orientation by the occipital bone to an organ culture chamber. The cylindrical piston applied cyclic forces with a sinusoidal waveform at 1 Hz and 200 mN to the sphenoid bone portion of the CBGP explant sample. The piston is a part of a hydraulic mechanical loading system (MTS MiniBionix) with computer control.

control and loaded explants were incubated in an organ culture chamber for three additional days with 95% air/5% CO₂ at 37°C. The control and loaded explants were cultured in the same chamber to ensure identical environment and nutrient supply.

2.3. Tissue processing and histology

The incubated samples were immediately fixed with 10% formalin overnight, and demineralized with 0.5 M EDTA. Once fully demineralized, the specimens were dehydrated in graded ethanol and xylene, and embedded in paraffin. Parasagittal sections were cut sequentially (5 µm thickness) with a microtome, and stained with hematoxylin and eosin (H&E) and safranin O/fast green.

2.4. Immunohistochemistry

Sequential sections were deparaffinized, washed in PBS, rehydrated with xylene and graded ethanol, and incubated for 30 min in bovine testicular hyaluronidase (1600 U/ml) in sodium acetate buffer (pH 5.5) with 150 mM sodium chloride. All immunohistochemical procedures using monoclonal antibodies (mAbs) followed our previous methods (Alhadlaq et al., 2004; Sundaramurthy and Mao, 2006; Tang and Mao, 2006). All primary and secondary antibodies are listed in Table 1. The same procedures were performed for negative controls except for the omission of the primary antibody.

2.5. Computer-assisted histomorphometry

The linear height of the CBGP explant was measured from six linear distances between the occipital and sphenoid bones using computerized histomorphometric analysis (Wang and Mao, 2002a). A grid system with a standard block size of 900 µm² was constructed over the entire CBGP at 20× magnification. The chondrocyte nuclei in each grid block were manually tagged, and automatically counted by image analysis software. The average total number of chondrocytes in six randomly selected grid blocks per specimen was calculated for each of the control specimens, whereas the average total number of hypertrophic chondrocytes in six grid blocks in the hypertrophic zone was calculated for each of the mechanically loaded specimens. The mAb binding was quantified as areas of mAb staining in six randomly selected grid blocks in the proliferative and hypertrophic zones, each from 10 randomly selected microscopic sections.

2.6. Biochemical assays

The loaded and control explants, upon the completion of three-day *ex vivo* incubation, were pooled, minced and forwarded for double-blinded biochemical assays. The samples were digested with papain. The DNA content was measured by bisbenzimidazole fluorescent (Hoechst 33258) using modified methods from our previous work (Alhadlaq et al., 2004). Briefly, the bisbenzimidazole fluorescent dye (Hoechst 33258) was used after digestion of the specimens with papain. The fluorescence of mixtures of the digested samples with Hoechst 33258 dye solution was determined

in duplicate using a spectrofluorometer. Fluorescence values were converted to DNA quantity using standards of DNA from calf thymus (Sigma, St. Louis, MO) in the appropriate buffer solution. The DNA content was converted to cellularity using the estimated value of 7.7 pg DNA per chondrocyte (Alhadlaq et al., 2004). Collagen content was measured by hydroxyproline assay using reversed-phase HPLC after hydrolysis with 6 M Hydrochloric acid for 16 h at 120°C and derivatization by phenylisothiocyanate (Dunphy et al., 1987). Briefly, hydroxyproline content was measured by phenylthiocarbonyl derivatization and isocratic reverse-phase high-performance liquid chromatography. After the derivatization by phenylisothiocyanate, the samples were separated isocratically using a reverse-phase C18 octadecylsilane column and monitored on an absorbance detector at 254 nm. Chondroitin sulfate and keratan sulfate contents were measured using a modified ELISA technique (Thonar et al., 1985). Purified bovine nasal septum was used as positive controls. Hyaluronic acid (HA) content was measured using a sandwich ELISA that detected HA strands with a relative molecular mass greater than 10,000 D (Li et al., 1989). A standardized solution of high molecular weight HA (Healon) was used to generate a standard curve. The counter stain was Mayer's hematoxylin for 3–5 min. The visualizing agent (DAB) was diaminobenzidine.

2.7. Data analysis and statistics

Upon confirmation of normal distribution, all numerical data were treated with Student *t*-tests to determine whether mechanically loaded specimens differed significantly from control specimens at an alpha level of *p*<0.05 with SPSS.

3. Results

Differences in structural characteristics of control and mechanically loaded growth plate explants were readily appreciable in microscopic sections. In contrast to abundant hypertrophic chondrocytes undergoing cell enlargement in the control explant (Fig. 2a), chondrocyte hypertrophy was not as prominent in the loaded specimen (Fig. 2b). Chondrocytes in the loaded specimens apparently were aligned into columnar-like structures (Fig. 2b), in contrast to a general lack of column-like arrangements of hypertrophic chondrocytes in the unloaded specimens (Fig. 2a). Both the control and loaded specimens were stained intensely to safranin O, indicating the abundance of chondroitin sulfate and keratan sulfate in cartilage matrix (Fig. 2c and d). The enlargement of chondrocytes and a general lack of columnar arrangements of hypertrophic chondrocytes superior to subchondral bone in the control explant were also appreciated by safranin O/fast green counterstain (Fig. 2c). In contrast, chondrocytes superior to subchondral bone in the loaded specimens were arranged into columns (Fig. 2d). The average number of chondrocytes per loaded specimen was 2685 ± 94/mm², significantly higher than the unloaded controls (1714 ± 221/mm²) (*p*<0.001) (Fig. 2e). The abundance of chondrocytes in loaded specimens was readily appreciated in Fig. 2b and d, in comparison with controls (Fig. 2a and c). The average linear height of the loaded specimens at 856 ± 30 µm was significantly higher than the unloaded controls at 830 ± 36 µm (*p*<0.05) (Fig. 2f).

Immunohistochemical localization of chondroitin sulfate, keratan sulfate, and versican showed remarkable

Table 1
Monoclonal antibodies used in immunolocalization of proteoglycans and glycosaminoglycans

Antibody	Chemical properties
Chondroitin sulfate (9BA12)	Carbohydrate epitope of chondroitin sulfate
Versican (12C5)	Protein epitope of versican
Keratan sulfate (I22)	Sulfated epitopes in keratan sulfate

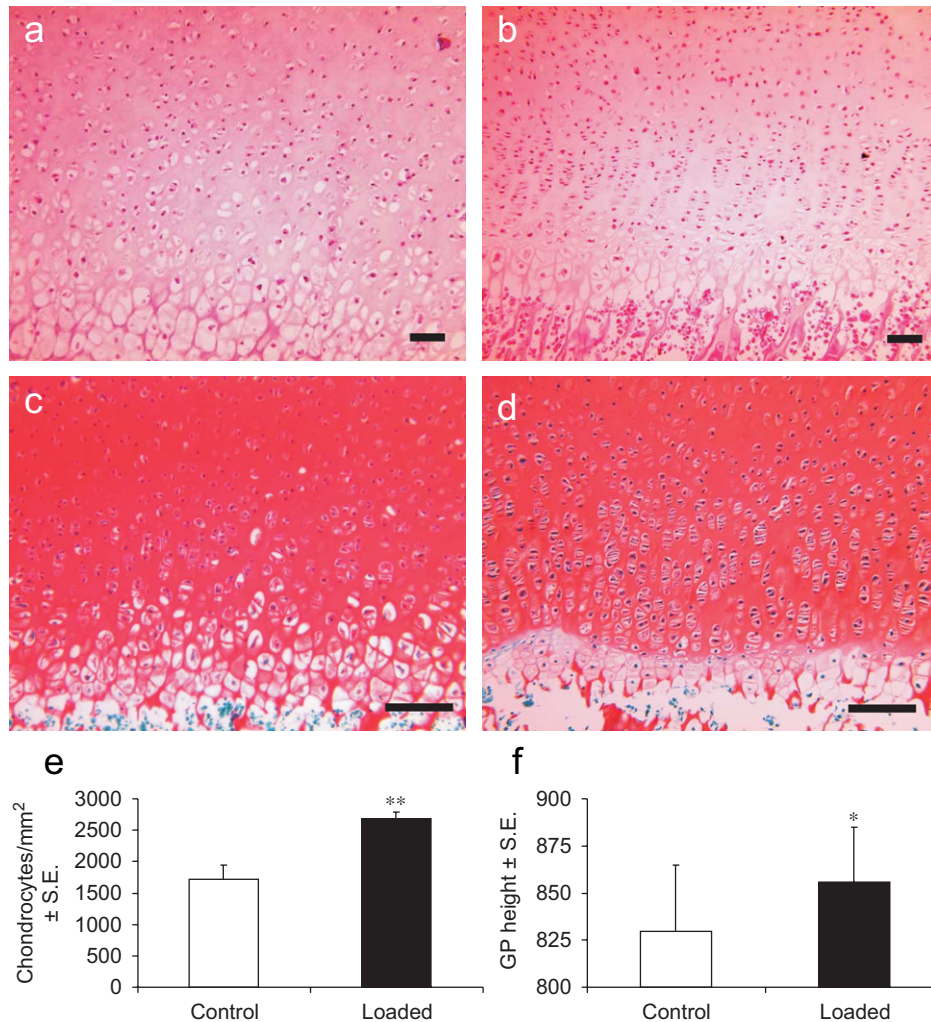


Fig. 2. Effects of cyclic loading on the structure and hypertrophy of growth plate samples, as well as on chondrocyte behavior. Safranin O staining for (a) through (d). (a) Control growth plate without mechanical loading demonstrates chondrocyte hypertrophy and no apparent column arrangement. (b) In contrast, mechanically loaded growth plate shows more defined column structures and less marked chondrocyte hypertrophy. The number of chondrocytes is qualitatively more marked than the control in (a). Scale bars in (a) and (b): 200 μm . (c) Higher magnification showing chondrocyte hypertrophy adjacent to tidemark. (d) Mechanically loaded growth plate sample showing minimal evidence of chondrocyte hypertrophy and abundance of chondrocytes in comparison to the control (c). (e) Quantification of the number of chondrocytes. The mechanically loaded growth samples had significantly more chondrocytes than unloaded controls ($p < 0.001$). (f) Quantification of total growth height. The average growth plate height of mechanically loaded samples was significantly higher than unloaded controls ($p < 0.05$). Scale bars in (c) and (d): 200 μm .

differences between the controls and loaded specimens. Chondroitin sulfate was expressed in the chondrocytes and areas of cartilage infiltration in subchondral bone in the unloaded controls (Fig. 3a1). In contrast, abundant chondroitin sulfate was expressed in chondrocytes superior to subchondral bone in the loaded specimen (Fig. 3a2). The average area of mAb binding for chondroitin sulfate was significantly higher in the loaded group at $10,560 \pm 1751 \mu\text{m}^2$ than the unloaded controls at $3444 \pm 469 \mu\text{m}^2$ ($p < 0.001$) (Fig. 3a). Keratan sulfate mAb binding appeared to be localized to hypertrophic chondrocytes superior to subchondral bone in the unloaded controls (Fig. 3b1), whereas mechanical loading induced marked expression of keratan sulfate superior to subchondral bone (Fig. 3b2). The average area of mAb

binding for keratan sulfate of the loaded specimens at $9853 \pm 1430 \mu\text{m}^2$ was significantly higher than the unloaded controls at $5843 \pm 1493 \mu\text{m}^2$ ($p < 0.01$) (Fig. 3b). Little versican mAb binding was found in the unloaded control specimen (Fig. 3c1), in comparison with somewhat marked versican expression in the loaded specimen (Fig. 3c2). This was confirmed by the quantification of versican mAb staining demonstrating that the average area of versican mAb staining for the loaded specimen at $7038 \pm 1355 \mu\text{m}^2$ was significantly higher than the unloaded control specimen at $5656 \pm 1103 \mu\text{m}^2$ (Fig. 3c).

The total hydroxyproline content as normalized to the total DNA content for the unloaded control group was $2.86 \pm 0.96 \mu\text{g}/\mu\text{g}$ DNA, lacking significant statistical differences to the average hydroxyproline content of

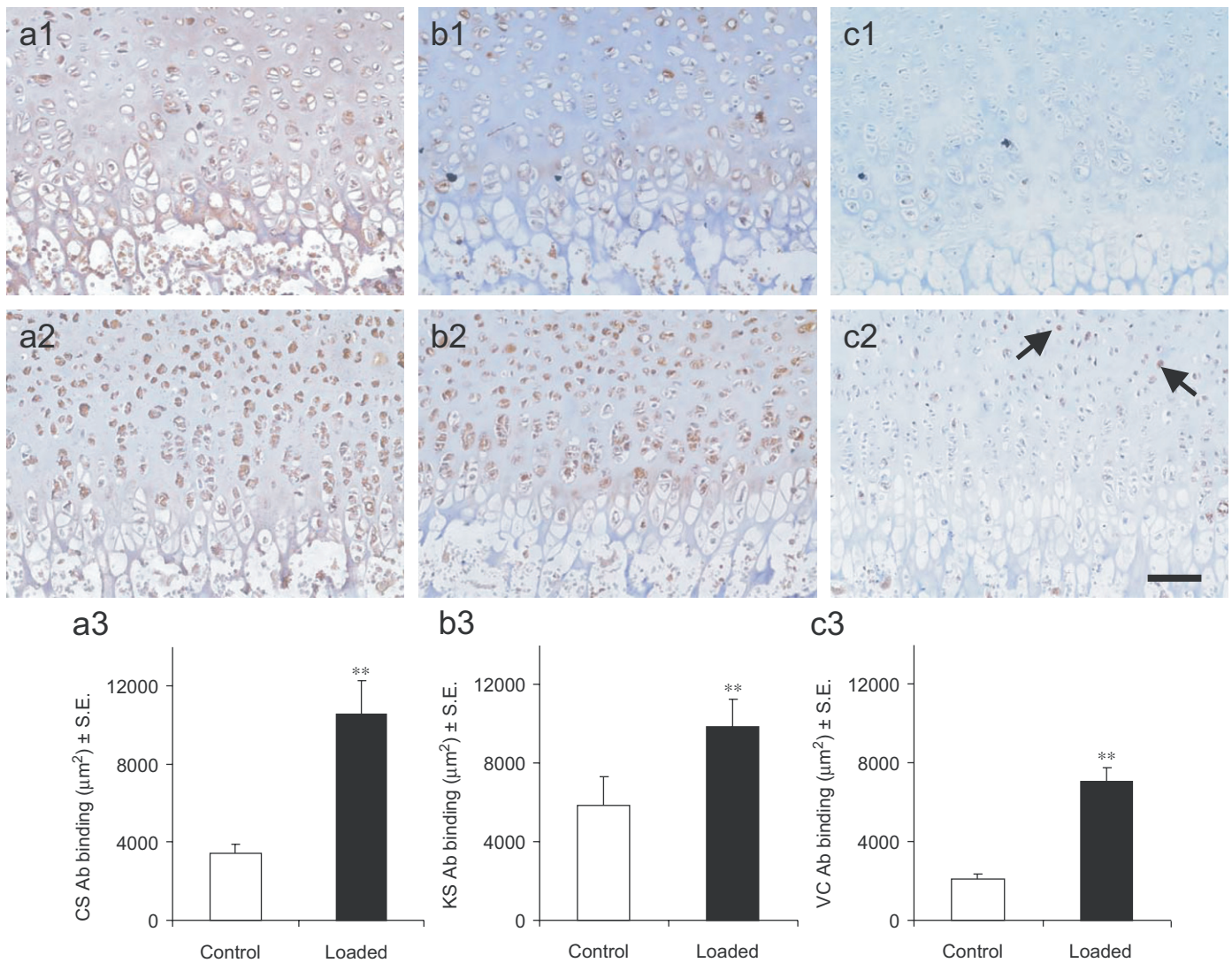


Fig. 3. Immunolocalization of growth plate samples by monoclonal antibodies. (a1) Unloaded control growth plate sample showing the expression of chondroitin sulfate primarily in the pericellular matrix. (a2) Mechanically loaded growth plate sample showing more abundant expression of chondroitin sulfate also primarily in the pericellular matrix. (a3) The average area of mAb binding for chondroitin sulfate was significantly higher in the mechanically loaded group at $10,560 \pm 1751 \mu\text{m}^2$ than the unloaded control group at $3444 \pm 469 \mu\text{m}^2$ ($p < 0.001$). (b1) Unloaded control growth plate sample showing the expression of keratan sulfate primarily in the pericellular matrix. (b2) Mechanically loaded growth plate sample showing more abundant expression of keratan sulfate also primarily in the pericellular matrix. (b3) The average area of mAb binding for keratan sulfate of the mechanically loaded specimen at $9853 \pm 1430 \mu\text{m}^2$ was significantly higher than the unloaded control specimen at $5843 \pm 1493 \mu\text{m}^2$ ($p < 0.01$). (c1) Little versican mAb binding was found in the unloaded control specimen. (c2) Versican expression (arrows) is more marked in the mechanically loaded specimen. Labeling is primary in the pericellular matrix. (c3) Quantification of versican mAb staining demonstrates that the average area of versican mAb staining for the mechanically loaded specimen at $7038 \pm 1355 \mu\text{m}^2$ was significantly higher than the unloaded control specimen at $5656 \pm 1103 \mu\text{m}^2$ ($p < 0.01$).

mechanically loaded specimens at $2.9 \pm 0.66 \mu\text{g}/\mu\text{g}$ DNA (Fig. 4a). The average total hyaluronan content of the loaded specimens at $0.25 \pm 0.06 \mu\text{g}/\mu\text{g}$ DNA was significantly higher than the average total hyaluronan content of the unloaded control group at $0.09 \pm 0.05 \mu\text{g}/\mu\text{g}$ DNA ($p < 0.01$) (Fig. 4b).

4. Discussion

These data represent an original demonstration of mechanical modulation of extracellular matrix molecules in the neonatal growth plate. The increases in chondrocyte

number, growth plate height and increased matrix molecule synthesis, appear to be consistent with previous findings of enhanced chondral growth upon the application of compressive forces, although loading is cyclic in the present study instead of static loading as in several models. *In vitro*, cyclic loading also has anabolic effects on chondrocytes and matrix synthesis (Li et al., 2004; Chao et al., 2005). Age difference may account for some of the discrepancies between the present neonatal growth plate loading and many previous studies. The present observation of enhanced column arrangement of hypertrophic chondrocytes in the neonatal growth plate upon cyclic loading

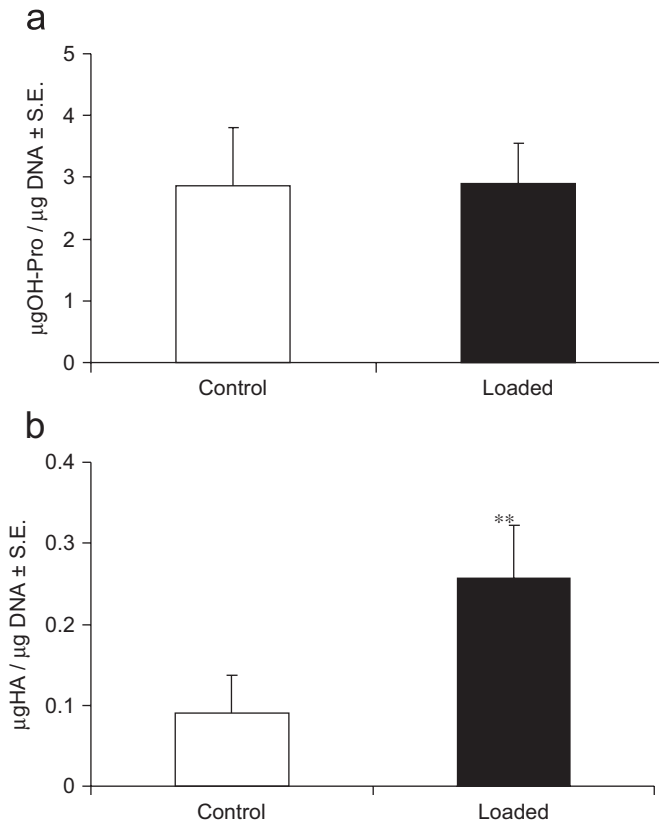


Fig. 4. Biochemical analysis. (a) The total hydroxyproline content as normalized to the total DNA content for the unloaded control group was $2.86 \pm 0.96 \mu\text{g}/\mu\text{g DNA}$, lacking statistically significant differences to the average hydroxyproline content of mechanically loaded specimens at $2.9 \pm 0.66 \mu\text{g}/\mu\text{g DNA}$. (b) The average total hyaluronan content of the mechanically loaded specimens at $0.25 \pm 0.06 \mu\text{g}/\mu\text{g DNA}$ was significantly higher than the average total hyaluronan content of the unloaded control group at $0.09 \pm 0.05 \mu\text{g}/\mu\text{g DNA}$ ($p < 0.01$).

indicates that mechanical stress at low magnitude may inhibit chondrocyte hypertrophy. In the CBGP, column arrangements of hypertrophic chondrocytes are present by 6 weeks of age (Wang and Mao, 2002a,b). In addition, the inhibition of chondrocyte hypertrophy is consistent with Wang and Mao (2002a, b).

The present demonstration of enhanced chondrocyte proliferation and matrix synthesis is consistent with increased glycosaminoglycans and DNA synthesis of chondrocytes isolated from the rabbit CBGP upon compressive loading. Our previous *in vivo* data showing increased growth plate height and cell density per growth plate area (Wang and Mao, 2002a, b) also using the rabbit model lend further support for the present *ex vivo* data. Additional studies are necessary to address the following issues. The duration of force applied in this study is 60 min and was selected on the basis of similar force parameters used in our previous studies of mechanical modulation of cranial sutures (Collins et al., 2005; Tang and Mao, 2006), as well as a companion study of mechanical modulation of neonatal distal femoral epiphysis (Sundaramurthy and Mao, 2006). Several other biomechanical issues should also

be addressed such as the effects of a duty cycle, e.g. 10 min on and 10 min off.

Force magnitude is likely of critical importance. Peak load of 200 mN likely represents a small fraction of the mechanical loads in other studies, e.g. up to 17 N applied to rat ulna growth plate *in vivo* (Robling et al., 2001; Ohashi et al., 2002). Growth suppression in association with high loads, such as 17 N (Robling et al., 2001; Ohashi et al., 2002), suggests that the yield strength of growth plate cartilage may have been reached. We previously found that ramp forces up to 10 N applied to human cadaver maxilla is transmitted as small bone strain adjacent to CBGP. Thus, it is unlikely that the present loading at 200 mN has induced growth suppression in the CBGP. The presently observed chondrocyte and matrix changes are responses to rather low force magnitude and do not conflict with the observation of suppression of chondral growth upon high loads (Ohashi et al., 2002; Robling et al., 2001). Collectively, whether chondrocyte's biological response is graded to force magnitude warrants additional investigations. Other mechanical parameters such as strain, pressure and fluid flow are also of interest. As designed, the study cannot distinguish separate actions of these parameters. Nonetheless, Due to the lack of *in vivo* environment in the present organ culture system, the effect of fluid flow would occur intrinsically in cartilage tissue without the contribution of perturbation of vascular supply in subchondral bone.

This *ex vivo* model, whilst advantageous for isolating the tested conditions, does not account for other factors that are important in cartilage development such as vascularization, growth hormone and other paracrine pathways. Strong reaction for chondroitin sulfate, keratan sulfate and versican in the pericellular matrix is in the area of the newly synthesized proteoglycans, apparently in agreement with highly labeled pericellular matrix using autoradiography. The present biochemical analysis failed to identify statistically significant differences in total glycosaminoglycans content. We attribute this to potential release of glycosaminoglycans into the culture medium upon mechanical loading. Biochemical analysis was the last experiment performed in the present project. This speculation needs to be clarified in additional experiments. The lack of statistically significant differences in total collagen content with or without mechanical loading can probably be accounted for by the probability that large type II collagen fiber synthesis is unaltered in the present *ex vivo* system in a short time.

The increased hyaluronan content upon cyclic loading is remarkable, and appears consistent with other recent findings. For example, mechanical stretch of uterine cervical fibroblast for up to 48 h significantly increases the secretion of HAS1, 2 and 3 (Takemura et al., 2005). Articular chondrocytes of 18-day chick embryos increase cell surface hyaluronan-binding protein expression and hyaluronan synthase mRNA expression during the minute mechanical stress resulting from movement in the primitive

fetal synovial joint (Dowthwaite et al., 1999). The roles of hyaluronan in mechanotransduction warrant additional investigations. Overall, the present basic science approach can perhaps be further explored for potential translation in clinical therapies in the correction of dentofacial deformities and craniofacial anomalies (Mao and Nah, 2004). For example, accelerated growth of the CBGP may lead to forward growth of the maxilla and midface, potentially useful for patients with midface deficiencies.

Acknowledgments

We are grateful to Lori Otten for her capable technical assistance with biochemical analysis. We thank two anonymous reviewers whose critical comments helped to improve the quality of the manuscript. This research was supported by NIH Grants DE13964 and DE15391 to J.J.M, and P50 AR-39239 and P01-AR48152 to E.J.T.

References

- Alhadlaq, A., Elisseff, J.H., Hong, L., Williams, C.G., Caplan, A.I., Sharma, B., Kopher, R.A., Tomkoria, S., Lennon, D.P., Lopez, A., Mao, J.J., 2004. Adult stem cell driven genesis of human-shaped articular condyle. *Annals of Biomedical Engineering* 32, 911–923.
- Alini, M., Roughley, P.J., 2001. Changes in leucine-rich repeat proteoglycans during maturation of the bovine growth plate. *Matrix Biology* 19, 805–813.
- Allen, D.M., Mao, J.J., 2004. Heterogeneous nanostructural and nanoelastic properties of pericellular and interterritorial matrices of chondrocytes by atomic force microscopy. *Journal of Structural Biology* 145, 196–204.
- Baume, L.J., 1961. Principles of cephalofacial development revealed by experimental biology. *American Journal of Orthodontics* 47, 881–901.
- Carter, D.R., Beupre, G.S., Giori, N.J., Helms, J.A., 1998. Mechanobiology of skeletal regeneration. *Clinical Orthopaedics Related Research* October (355 Suppl.), S41–S55.
- Chao, P.G., Tang, Z., Angelini, E., West, A.C., Costa, K.D., Hung, C.T., 2005. Dynamic osmotic loading of chondrocytes using a novel microfluidic device. *Journal of Biomechanics* 38, 1273–1281.
- Dowthwaite, G.P., Ward, A.C., Flannely, J., Suswillo, R.F., Flannery, C.R., Archer, C.W., Pitsillides, A.A., 1999. The effect of mechanical strain on hyaluronan metabolism in embryonic fibrocartilage cells. *Matrix Biology* 18, 523–532.
- Dunphy, M.J., Bhide, M.V., Smith, D.J., 1987. Determination of hydroxyproline in tissue collagen hydrolysate by derivatization and isocratic reversed-phase high-performance liquid chromatography. *Journal of Chromatography* 420, 394–397.
- Farnum, C.E., Nixon, A., Lee, A.O., Kwan, D.T., Belanger, L., Wilsman, N.J., 2000. Quantitative three-dimensional analysis of chondrocytic kinetic responses to short-term stapling of the rat proximal tibial growth plate. *Cells Tissues Organs* 167, 247–258.
- Farnum, C.E., Lee, A.O., O'Hara, K., Wilsman, N.J., 2003. Effect of short-term fasting on bone elongation rates: an analysis of catch-up growth in young male rats. *Pediatric Research* 53, 33–41.
- Grodzinsky, A.J., Levenston, M.E., Jin, M., Frank, E.H., 2000. Cartilage tissue remodeling in response to mechanical forces. *Annual Review of Biomedical Engineering* 2, 691–713.
- Hoyte, D.A., 1991. The cranial base in normal and abnormal skull growth. *Neurosurgery Clinics of North America* 2, 515–537.
- Ingervall, B., Thilander, B., 1972. The human sphenoccipital synchondrosis I. The time of closure appraised macroscopically. *Acta Odontologica Scandinavica* 30, 349–356.
- Kirsch, T., Nah, H.D., Shapiro, I.M., Pacifici, M., 1997. Regulated production of mineralization-competent matrix vesicles in hypertrophic chondrocytes. *Journal of Cell Biology* 137, 1149–1160.
- Klein-Nulend, J., Veldhuijzen, J.P., Burger, E.H., 1986. Increased calcification of growth plate cartilage as a result of compressive force in vitro. *Arthritis and Rheumatism* 29, 1002–1009.
- Kopher, R.A., Mao, J.J., 1999. Suture growth modulated by the oscillatory component of micromechanical strain. *Journal of Bone and Mineral Research* 18, 521–528.
- Li, X., Thonar, E., Knudson, W., 1989. Accumulation of hyaluronate in human lung carcinoma as measured by a new hyaluronate ELISA. *Connective Tissue Research* 19, 243–253.
- Li, K.W., Klein, T.J., Chawla, K., Nugent, G.E., Bae, W.C., Sah, R.L., 2004. In vitro physical stimulation of tissue-engineered and native cartilage. *Methods in Molecular Medicine* 100, 325–352.
- Mao, J.J., Nah, H.D., 2004. Growth and development: hereditary and mechanical modulations. *American Journal of Orthodontics and Dentofacial Orthopedics* 125, 676–689.
- Mao, J.J., 2005. Calvarial development: cells and mechanics. *Current Opinion in Orthopedics* 16, 331–337.
- Mao, J.J., Rahemtulla, F., Scott, P.G., 1998. Proteoglycan expression in the rat temporomandibular joint in response to unilateral bite raise. *Journal of Dental Research* 77, 1520–1528.
- Nilsson, O., Baron, J., 2004. Fundamental limits on longitudinal bone growth: growth plate senescence and epiphyseal fusion. *Trends in Endocrinology and Metabolism* 15, 370–374.
- Ohashi, N., Robling, A.G., Burr, D.B., Turner, C.H., 2002. The effects of dynamic axial loading on the rat growth plate. *Journal of Bone Mineral Research* 17, 284–292.
- Peltomaki, T., Kylamarkula, S., Vinkka-Puhakka, H., Rintala, M., Kantomaa, T., Ronning, O., 1997. Tissue-separating capacity of growth cartilages. *European Journal of Orthodontics* 19, 473–481.
- Proffit, W.R., Fields, H.W., Ackerman, J.L., Bailey, L., Tulloch, J.F.C., 2000. *Contemporary Orthodontics*. Mosby Year Book, St Louis, pp. 295–362.
- Radhakrishnan, P., Mao, J.J., 2004. Nanomechanical properties of facial sutures and sutural mineralization front. *Journal of Dental Research* 83, 470–475.
- Robling, A.G., Duijvelaar, K.M., Gevers, J.V., Ohashi, N., Turner, C.H., 2001. Modulation of appositional and longitudinal bone growth in the rat ulna by applied static and dynamic force. *Bone* 29, 105–113.
- Rosenberg, P., Arlis, H.R., Haworth, R.D., Heier, L., Hoffman, L., LaTrenta, G., 1997. The role of the cranial base in facial growth: experimental craniofacial synostosis in the rabbit. *Plastic and Reconstructive Surgery* 99, 1396–1407.
- Scott, J., 1958. The cranial base. *American Journal of Physical Anthropology* 16, 319–348.
- Stokes, I.A., Mente, P.L., Iatridis, J.C., Farnum, C.E., Aronsson, D.D., 2002. Enlargement of growth plate chondrocytes modulated by sustained mechanical loading. *Journal of Bone and Joint Surgery American* 84-A, 1842–1848.
- Stokes, I.A., Gwadera, J., Dimock, A., Farnum, C.E., Aronsson, D.D., 2005. Modulation of vertebral and tibial growth by compression loading: diurnal versus full-time loading. *Journal of Orthopedic Research* 23, 188–195.
- Sundaramurthy, S., Mao, J.J., 2006. Mechanical modulation of endochondral development in the distal femoral condyle. *Journal of Orthopedic Research* 24, 229–241.
- Takemura, M., Itoh, H., Sagawa, N., Yura, S., Korita, D., Kakui, K., Kawamura, M., Hirota, N., Maeda, H., Fujii, S., 2005. Cyclic mechanical stretch augments hyaluronan production in cultured human uterine cervical fibroblast cells. *Molecular Human Reproduction* 11, 659–665.
- Tanck, E., van Driel, W.D., Hagen, J.W., Burger, E.H., Blankevoort, L., Huiskes, R., 1999. Why does intermittent hydrostatic pressure enhance the mineralization process in fetal cartilage? *Journal of Biomechanics* 32, 153–161.
- Tang, M., Mao, J.J., 2006. Matrix and gene expression in the rat cranial base growth plate. *Cell and Tissue Research* 324, 467–474.

- Thonar, E., Lenz, M., Klintworth, G., Caterson, B., Pachman, L., Glickman, P., Katz, R., Huff, J., Kuettner, K., 1985. Quantification of keratan sulfate in blood as a marker of cartilage catabolism. *Arthritis and Rheumatism* 28, 1367–1376.
- Van der Eerden, B.C., Karperien, M., Wit, J.M., 2003. Systemic and local regulation of the growth plate. *Endocrine Reviews* 24, 782–801.
- Wang, X., Mao, J.J., 2002a. Accelerated chondrogenesis of the rabbit cranial base growth plate by oscillatory mechanical stimuli. *Journal of Bone and Mineral Research* 17, 1843–1850.
- Wang, X., Mao, J.J., 2002b. Chondrocyte proliferation of the cranial base cartilage upon in vivo mechanical stresses. *Journal of Dental Research* 81, 701–705.